Selective optical detection of H_2 and CO with SiO_2 sol gel films containing NiO and Au nanoparticles

Buso, D.; Busato, G.; Guglielmi, M.; Martucci, A.; Bello, V.; Mattei, G.; Mazzoldi, P.; Post, M. L.

Publisher's version / Version de l'éditeur:
https://doi.org/10.1088/0957-4484/18/47/475505
Nanotechnology, 18, 47, pp. 475505-1-475505-7, 2007-10-26

Selective optical detection of H_2 and CO with SiO_2 sol–gel films containing NiO and Au nanoparticles

2007 Nanotechnology 18 475505

(http://iopscience.iop.org/0957-4484/18/47/475505)

Nanotechnology **18** (2007) 475505 (7pp) doi:10.1088/0957-4484/18/47/475505

Selective optical detection of H_2 and CO with SiO_2 sol–gel films containing NiO and Au nanoparticles

D Buso[1], G Busato[1], M Guglielmi[1], A Martucci[1], V Bello[2], G Mattei[2], P Mazzoldi[2] and M L Post[3]

[1] Dipartimento di Ingegneria Meccanica–Settore Materiali, Università di Padova, via Marzolo, 9, I-35131 Padova, Italy
[2] Dipartimento di Fisica, Università di Padova, via Marzolo 8, I-35131 Padova, Italy
[3] Institute for Chemical Process and Environmental Technology, National Research Council of Canada, 1200 Montreal Road, Ottawa, ON, K1A 0R6, Canada

Received 22 August 2007, in final form 21 September 2007
Published 26 October 2007
Online at stacks.iop.org/Nano/18/475505

Abstract
NiO is a p-type semiconductor widely studied for its promising implementation in chemo-optical gas sensors. Reducing/oxidizing gases induce a change in optical absorption of NiO. It has been found that Au doping induces a remarkable increase in the NiO sensitivity, and at the same time silica films obtained by the sol–gel technique have been demonstrated to be a suitable support matrix for gas-sensitive materials due to their extremely high specific surface area (up to 600 $m^2\ g^{-1}$). The aim of this work is the synthesis of SiO_2 films containing both NiO and Au nanoparticles and their morphological and functional characterization as active gas-sensing materials suitable for optical detectors. The possibility to selectively recognize H_2 and CO is studied exploiting the wavelength dependence of the gas-induced optical transmittance variation.

1. Introduction

The application of nanostructured materials in the design of new gas-sensing devices is presently one of the most dynamic research issues, due to the possibility of increasing the sensing performance by exploiting the high activity, large specific surface and small size of active materials [1]. Environmental control requires reliable, high performance sensing devices with good sensitivity, selectivity and stability, a combination of desirable features which is not always attained. In addition to offering significant advantages over electric-conductometric devices in some circumstances [2, 3], optical gas sensors present a new class of special parameters that can be exploited to tailor the sensing behaviour towards specific target gases [4]. For many years hydrogen gas has been used as a reducing agent in the chemical industry as well as a carrier gas in semiconductor manufacturing processes [5], and recently there has been increased interest towards its employment as a clean energy resource through fuel cell technology and other hydrogen-based energy vectors. Therefore selective detection of H_2 has been a focus of materials research for some time. Conductometric sensors based on semiconductors can have improved selectivity by means of filtering [6, 7] or by adding catalytic layers [8], but these steps increase device complexity and also can cause a deterioration of sensor response rate. Direct recognition of target gases can potentially be achieved by using optical gas sensors, and in particular for cases where the gas-induced variation of the monitored optical parameter shows a clear wavelength dependence, as has been demonstrated by Ando *et al* using an Au–Co_3O_4 film [9]. This concept has been expanded in the present work to modulate the detection of either CO and H_2, and to reduce CO interference when detecting H_2 by means of using the optical transmittance properties of sol–gel SiO_2 films containing Au and NiO nanoparticles.

2. Experimental details

SiO_2 films containing Au and NiO nanoparticles were synthesized using tetraethoxy silane (TEOS), methyl-triethoxy silane (MTES), H_2O, HCl in EtOH solution as SiO_2 precursors, and $HAuCl_4$ and $NiCl_2{\cdot}6H_2O$ as Au and NiO precursors

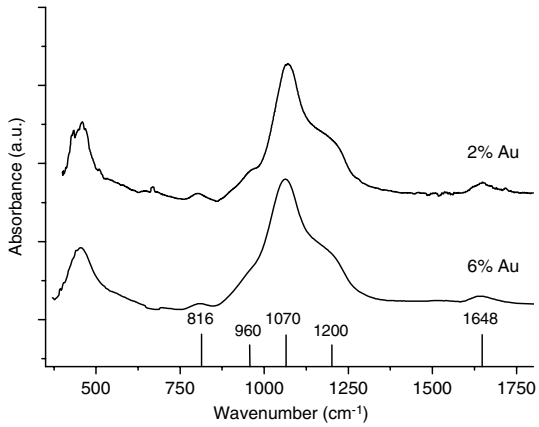

Figure 1. FTIR spectra of samples with 2% and 6% molar Au content after annealing at 500 °C. Main spectra features associated with SiO_2 network structure are marked at the bottom.

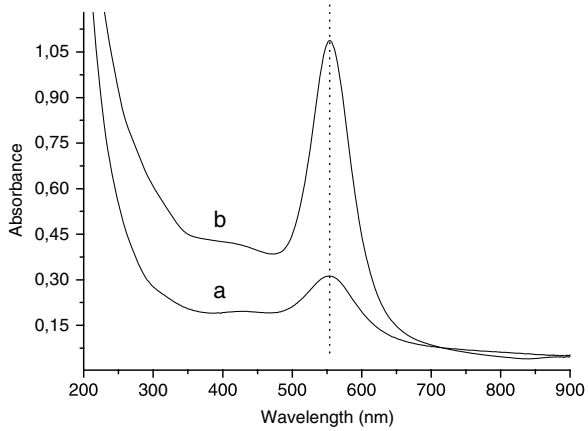

Figure 2. Room temperature optical absorption spectra of SiO_2 films containing (a) 2% and (b) 6% Au.

according to a method described elsewhere [4]. N-[3-(trimethoxysilyl)propyl]-ethylenediammine (DAEPTMS) was employed as a coordinating agent using DAEPTMS:Ni = 1:1 molar ratio. Films with Ni:Au ratios of 5 and 15 were synthesized in order to obtain a nominal Au content of 6% and 2% (molar), respectively. Moreover the amount of Ni precursor used was tailored to obtain a final composite with a SiO_2:NiO ratio of 7:3 (70% SiO_2–30% NiO molar). Optically cleaned SiO_2 substrates were *dip-coated* using 120 cm min^{-1} withdrawal speed through a deposition process performed at 23 °C under a constant RH% environment (25%). Sample films subsequently underwent thermal treatments at 500 °C for 30 min.

Infrared spectroscopy (FTIR) was performed in the 400–4000 cm^{-1} range using a Perkin-Elmer 2000 System instrument. Optical absorption spectra of samples were measured in the 300–900 nm range using a Jascow V-570 standard spectrophotometer.

Structural and compositional characterization was performed on cross-sectional samples of the composite films. Measurements were taken with a field emission FEI TECNAI F20 SuperTwin FEG-(S)TEM microscope operating at 200 kV and equipped with an EDAX energy-dispersive x-ray spectrometer (EDS) for compositional analysis and a Gatan 794 Multiple Scan Camera, allowing digital image recording on a 1024 × 1024 pixel CCD array.

Optical sensor functionality was studied by making optical absorbance/transmittance measurements over the wavelength range 350 nm $< \lambda <$ 800 nm with sample films mounted on a heater inside a custom-built gas flow cell coupled with a Varian Cary1E spectrophotometer. Films heated at temperatures between room temperature and 330 °C were exposed to different concentrations of H_2 and CO in dry air. The substrate size was approximately 1 cm × 2 cm and the incident spectrophotometer beam was normal to the film surface and covering a 6 mm × 1.5 mm section area.

3. Results and discussion

FTIR analysis was used to qualitatively describe the main features of the SiO_2 matrix. Figure 1 reports FTIR spectra of SiO_2 films containing Au and NiO nanoparticles at both 2% and 6% Au concentrations. The main peak centred in the 1060–1080 cm^{-1} range is associated with antisymmetric stretching vibrations (TO_3 modes) of Si–O bonds in Si–O–Si groups inside the SiO_2 network [10], while the wide shoulder centred around 1200 cm^{-1} refers to the LO_3 stretching modes of Si–O–Si bonds, activated by scattered IR radiation within the pore walls [10]. Peaks at 816 cm^{-1} are referred to symmetric stretching (or bending [11]) motion (TO_2) of oxygen atoms in Si–O–Si bonds [10]. Signals at 960 cm^{-1} and 1648 cm^{-1} can be attributed to stretching of non-bridging oxygen atoms (e.g. unreacted Si–OH groups) [11] and weak bending vibration of H–O–H in H_2O [12], respectively. Densification of the SiO_2 network induced by thermal annealing can be monitored through the position of the main Si–O–Si vibration signal [13], thus obtaining a relative scale of film porosity. A peak centre shift from 1062 cm^{-1} to 1070 cm^{-1} is registered for films containing 6% and 2% of Au, respectively, acceptably explained by a decrease of matrix densification induced by a higher amount of Au precursor in the starting solution. Chemistry of sol–gel hydrolysis and condensation is strongly affected by the pH of the precursor sol, and acidic conditions in particular lead to a severe limitation of the polycondensation reactions. Only the rapid evaporation of the solvent during the deposition process would trigger condensation phenomena and a porous gel film would form, thus permitting the tailoring of the matrix structure through control of the weight distribution of oligomers present in the solution [10]. It is therefore clear that different pH levels lead to different mass oligomers in solution which affects the final degree of densification of the deposited matrix. The presence of unreacted residual silanol groups after annealing, evidenced by FTIR spectra, further attests to this assertion. Thus, it is reasonable to consider that the lower pH due to a higher amount of $HAuCl_4$ in solution causes the lower degree of densification of the SiO_2 network observed in FTIR spectra.

After the annealing procedure the films appear transparent and pinkish in colour, this observation evidenced in the optical absorption spectra reported in figure 2. Absorbance in the visible range is dominated by a strong band centred at 553 nm (room temperature) that is associated with the surface

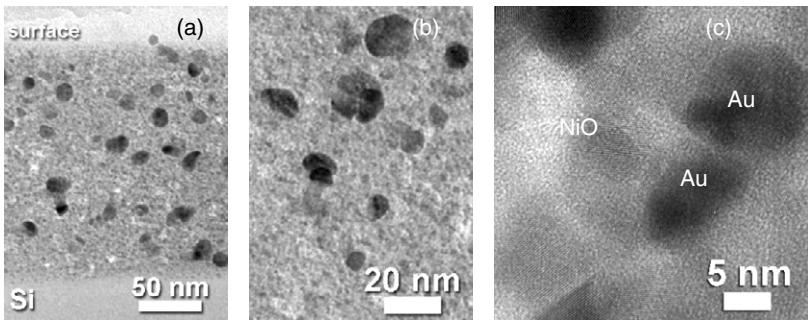

Figure 3. Cross-sectional TEM (a), (b) and HRTEM (c) images of SiO_2 matrix containing Au and NiO nanoparticles.

plasmon resonance (SPR) of conduction electrons on gold cluster surfaces. It is well known [14] from the Mie theory that the SPR frequency of metallic Au clusters is strongly affected by the dielectric nature of the hosting media, and this relationship can be helpfully exploited to get information about the structure of the immediate surroundings of gold nanoparticles [15]. Using optical constants for metallic gold evaluated by Johnson and Christy [16] (reliable for Au clusters of less than 60 nm in diameter [17], and found to be very accurate for the $1.3 < n < 1.7$ range in fluids [18]), it is possible to estimate the refractive index of the Au cluster surroundings by means of the wavelength and cluster-size-dependent formula proposed by Scaffardi *et al* [19]. The mean Au particle diameter estimated from TEM images of figure 3 was determined to be 11.9 nm (2.3 nm SD). Furthermore, SPR bands are centred at 553 nm for both Au concentrations. Implementing these values in the Scaffardi *et al* formula, the value of n of the dielectric environment hosting the Au nanoparticles was found to be 1.64. An explanation of this value can be deduced from the TEM pictures of figure 3.

Figures 3(a) and (b) show a cross-sectional image of the SiO_2 film containing dispersed Au clusters (dark spots) all throughout the film thickness. Moreover the HRTEM image of figure 3(c) shows that Au clusters are immersed in the SiO_2 matrix and finely surrounded by small crystalline aggregates of NiO. The refractive index value calculated for the Au host media (1.64) is higher than the well-known value of n for pure dense SiO_2 (1.46 [10]), but acceptable if it is considered that the dielectric nature of the matrix surrounding the Au clusters is affected also by the presence of NiO nanoclusters, as shown in the HRTEM image. The refractive index of crystalline NiO is reported to be in the 2.26–2.45 range [20, 21], thus giving a plausible explanation of the higher n calculated for the Au hosting media from optical spectra. The nature of the aggregates was determined by fast Fourier transform (FTT) and EDX quantitative analysis after focusing the electron beam on the regions of interest in the clusters visible in the HRTEM images. The region with darker contrast shows lattice fringes of fcc Au(111) planes ($d_{111} = 0.236$ nm), whereas a second periodicity arising from the region with brighter contrast can be indexed as coming from NiO fcc (200) planes ($d_{200} = 0.207$ nm).

EDX quantitative analysis was performed on specimen areas visible in TEM and HRTEM images of figures 3(a)–(c). The Ni/Au ratio was found to be 4.1 ± 0.5 and 11 ± 1 for films with nominal Au concentration of 2% and 6%, respectively, slightly lower than the nominal values adopted in the sample preparation recipe but with the same order of magnitude.

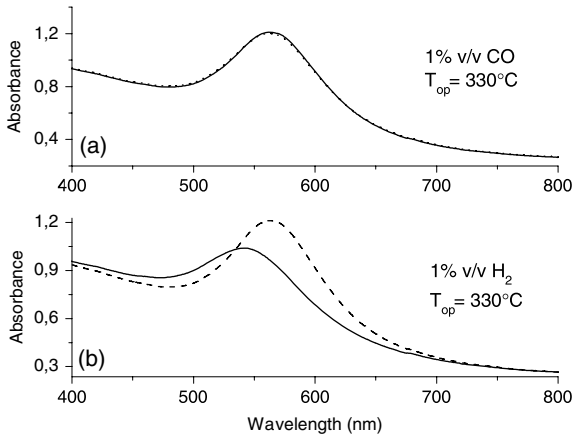

Figure 4. Optical absorption spectra measured at 330 °C in air (dotted lines) and after (a) 1% v/v CO and (b) 1% v/v H_2 exposure. The spectra refer to a sample with 6% Au content.

Functional optical characterization demonstrated that reducing species such as CO and H_2 produce a reversible variation of optical transmittance suitable for gas-sensing applications.

The effect of the different gaseous species on the optical properties of the samples can be seen in figure 4 which reports the optical absorbance spectra of films measured in air and under gas exposure (1% CO or H_2 at 330 °C on samples with 6% Au). SPR bands appearing in spectra taken in air at 330 °C are redshifted with respect to the bands observed in spectra measured at room temperature (figure 2). Temperature dependence of SPR frequencies is a known feature of plasmon bands [22]. The SPR band of the SiO_2–NiO–Au film is not appreciably modified by 1% v/v CO in either wavelength or band shape, an observation described in earlier work [4]. However, it is shifted and less intense in the case of exposure to H_2 under the same operative conditions. At 330 °C, 1% v/v of H_2 blueshifts the SPR band from 563 to 541 nm, thereby reducing the calculated refractive index of the hosting media from 1.75 to 1.49 (calculated values refer strictly to the immediate surroundings of Au nanoparticles).

To explain the influence of gold nanoparticles on the detection mechanism of transition metal oxides, two types of effects have been proposed [23]. *Type 1* is related to

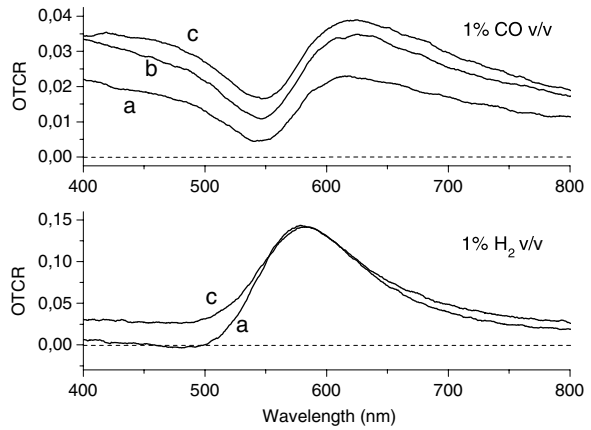

Figure 5. Optical transmittance change ratio (OTCR) induced by 1% CO v/v and 1% H_2 v/v in SiO_2–NiO–Au containing 2% Au measured in the whole visible range. Operating temperatures: (a) 230 °C, (b) 280 °C and (c) 330 °C.

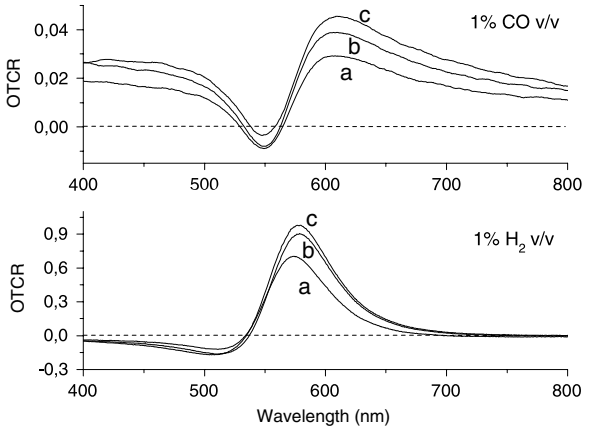

Figure 6. Optical transmittance change ratio (OTCR) induced by 1% CO v/v and 1% H_2 v/v in SiO_2–NiO–Au containing 6% Au measured in the whole visible range. Operating temperatures: (a) 230 °C, (b) 280 °C and (c) 330 °C.

an increased catalytic activity promoted by gold, closely associated with the catalytic activity of the Au–transition metal oxide composite [24]. In *type 2* the enhancement arises from the plasmon absorption change of Au particles, which is not directly related to the catalytic oxidation. As reported above, SPR frequencies are strongly influenced by the physical properties of the surrounding material such as dielectric constants. A gas-induced variation of these properties would affect both wavelength and shape of the SPR band of gold particles, as already observed in Au–CuO [23, 25] films when exposed to CO.

The strong variation in SPR band shape and position observed for H_2 exposure suggests that the sensing mechanism in H_2 detection is probably related to *type 2* sensing effect, in contrast to observations summarized by Ando *et al* for NiO–Au systems [25]. In either case, however, a more detailed understanding of the electronic structure of the particles in the presence of the gas and the role of the excited electronic plasma on the Au nanoparticles' surface during reaction with a target gas are crucial to provide a more detailed description of the detection mechanism.

In the case of optical CO detection at SPR band frequencies, a possible mechanism could be related to injection of electrons from NiO into gold nanoparticles during CO exposure, which would decrease the number of electrons available at the NiO surface involved in the reaction. This in turn would lead to a reduction in the number of reacting gas molecules and to an increase of conducting electrons involved in the plasmon resonance [26]. In their study on thin Au films deposited on a transparent NiO layer Matsubara *et al* [27] report that the evanescent wave from the metal oxide was effectively absorbed by the surface plasmon of the thin metal film at the interface. This suggests that the absorbance decrease of NiO induced by CO might be compensated by the plasmon band absorption of the small Au particles, thus leading to an overall increase of the material absorbance in the SPR frequencies. It should be pointed out that for NiO–Au systems a CO induced absorbance increase was observed, while only a decrease in optical absorbance in the plasmon band region has been observed before [25, 28, 29]. The present data indicates that no Au–NiO interface formation was observed, and electronic tunnelling effects through the energy barrier imposed by the SiO_2 walls between the two species can be postulated to support these explanations.

Plots reported in figures 5 and 6 show the transmittance variation registered after exposing all the samples to 1% v/v CO and 1% v/v H_2 in dry air for 5 min. The optical transmission variation is plotted in terms of optical transmittance change ratio (OTCR), defined as $[Tr_{1\%\ v/v\ CO} - Tr_{dry\ air}]/Tr_{dry\ air}$, as a function of the wavelength. This definition was given to overcome any differences in transmitted signal that could arise from inhomogeneities in film thickness, unequal reflectance ratios of the measuring beam and calibration discrepancies that could easily produce artefacts. The plots refer to tests performed at temperatures in the 230–330 °C range, and OTCR values showed wavelength and temperature dependence in all cases. Plots show a strong discontinuity in the SPR band frequencies (500–650 nm), with opposite characteristics depending on the gas nature. CO induces a clear depression in OTCR trends with a minimum around 545 nm while H_2, in contrast, confers to the OTCR profile a sharp positive peak centred at 580 nm. Higher operative temperatures lead to an increase of OTCR in the overall spectral range, demonstrating that sensing kinetics for SiO_2–Au–NiO films is thermally promoted. The reason for the differences in the OTCR spectra is still to be clarified, but it certainly implies a difference in sensing mechanism towards each of the two gaseous species.

Figure 7 presents a direct comparison of gas-sensing performance for samples containing different Au amounts towards CO and H_2. The maximum OTCR values registered for each sample are plotted as a function of the operative temperature in a logarithmic scale, showing in all cases a temperature-promoted sensing capability. In detecting the same gaseous species, samples with 6% gold content display a higher response level in all conditions, thus providing higher OTCR maximum values. The high sensing capability of the films toward H_2 detection is therefore evident, and almost double values of optical transmittance (%) compared to values in air were registered when detecting 1% H_2 v/v at 330 °C

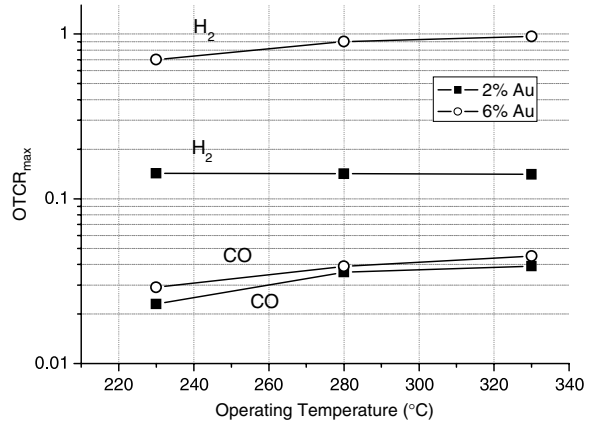

Figure 7. OTCR maximum values according to operating temperature observed after exposure to 1% v/v CO and 1% v/v H_2 in dry air.

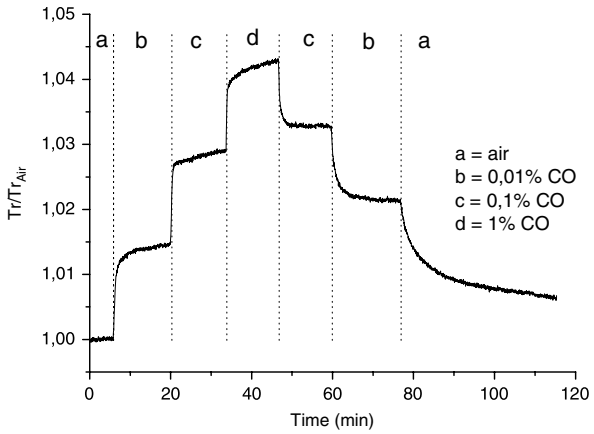

Figure 8. Temporal response of a film containing 2% Au as a function of CO concentration in air measured at $\lambda = 625$ nm and $T_{op} = 330\,^{\circ}$C for films with 6% Au content.

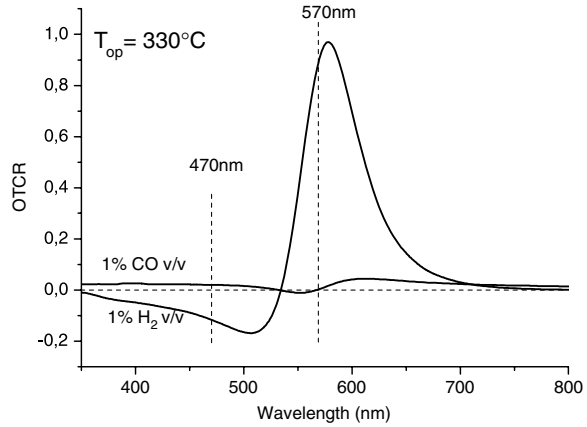

Figure 9. Comparison between OTCR values induced by 1% CO and 1% H_2 measured at $T_{op} = 330\,^{\circ}$C for films with 6% Au content. Vertical dotted lines depict wavelengths at which the films have been further tested to get dynamic responses reported in figures 10 and 11.

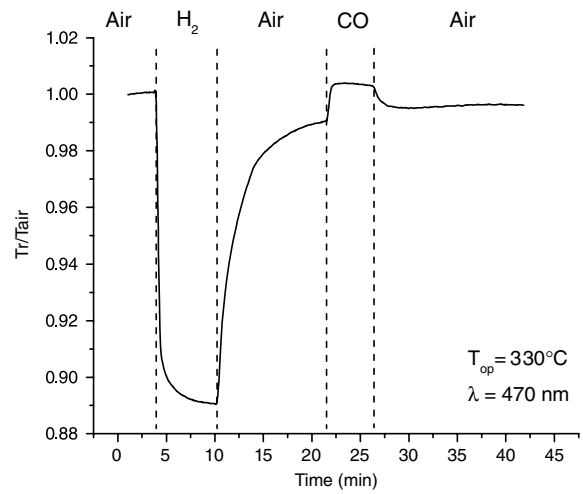

Figure 10. Dynamic response of film containing 6% Au exposed to air–1% H_2 v/v–air–1% CO v/v cycles. The test was performed at 330 °C and optical transmittance recorded at 470 nm.

with the sample containing 6% of Au (OTCR = 0.97). The maximum OTCR measured in CO detection was substantially lower at about 0.045.

In order to evaluate the sensor sensitivity the films have been exposed to different concentrations of CO and H_2. The films gave detectable responses in dynamic tests with a minimum concentration of 0.01% v/v of both H_2 and CO. As an example, figure 8 shows transmittance data obtained at $\lambda = 625$ for a film containing 2% Au at an operating temperature of 330 °C for three CO concentrations in air (0.01%, 0.1%, and 1% v/v). Clearly a CO concentration dependence is evident, and transmittance changes are easily observable even at concentrations of 0.01% CO. The relative transmittance changes, based on the initial (air) baseline, are 1.4%, 2.8% and 4.2% for 0.01%, 0.1% and 1% CO in air, respectively, indicating a log concentration dependence on transmittance response.

The strong wavelength dependence of OTCRs and the difference between OTCR values measured for H_2 and CO exposure allows modulation of the film response towards each of the two species. Figure 9 reports a comparison between OTCR values registered when exposing a film with 6% Au content to 1% CO (v/v) and 1% H_2 (v/v) at 330 °C. Wavelength dependence of OTCR values is evident, and once again the high sensitivity of this material towards H_2 detection over CO is clear. However, it is possible to modulate the sensing capability of the film by simply varying the wavelength at which dynamic responses toward gases are recorded. Figure 9 shows, for example, that at 470 nm the OTCR value for CO detection is positive while it is negative for H_2. Therefore a negative drop of transmittance should be expected when exposing the film to H_2, and a positive inflection in the case of CO exposure. This is further demonstrated by the dynamic response reported in figure 10, which refers to the optical transmittance evolution in time of a film with 6% Au content exposed to air–1% H_2 (v/v)–air–1% CO (v/v) cycles at 330 °C. Negative and positive variations of optical transmittance induced either by H_2 and CO, respectively, are evident.

The even more appealing possibility to switch detection towards only one of the two species is also possible. A

Table 1. CO-and H_2-induced modification in optical absorbance of several Au–metal oxide systems observed in the SPR band spectral region (500–650 nm).

Material	Target gases	Tested operative temperature (°C)	Absorbance change observed in SPR region	Observed shift in SPR band wavelength	Reference
SiO_2–NiO–Au	CO H_2	200–330	Increase Decrease	No Yes	Present work
Au–NiO	CO	150–250	Decrease	No	[25, 28, 29]
Au–CuO	CO	225–300	Increase	Yes	[23, 25]
Au–Co_3O_4	CO H_2	200	Decrease Increase	No No	[9, 25]
Au–WO_3	H_2	200–250	Increase	No	[30]
Au–$In_xO_yN_z$	H_2	200–300	Increase	Yes	[22]

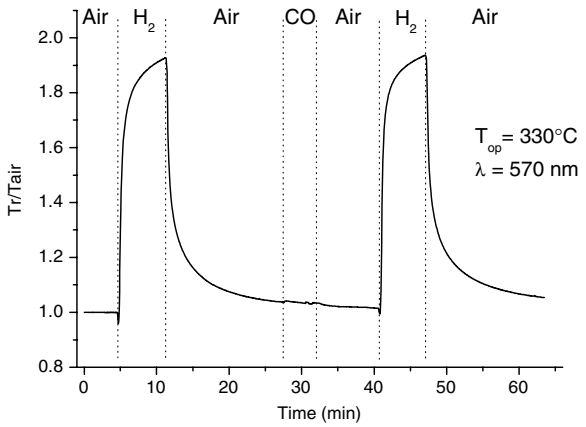

Figure 11. Dynamic response of SiO_2–NiO–Au film containing 6% Au exposed to air–1% v/v H_2–air–1% v/v CO cycles. Measurements performed at 330 °C and optical transmittance recorded at 570 nm. Interference of 1% v/v CO evaluated.

dynamic response performed at 570 nm, as shown in figure 9 again, should virtually exclude CO from detection. Indeed the dynamic response reported in figure 11 confirms it. It reports the time evolution of optical transmission, measured at 570 nm, of a film with 6% Au content when exposed to sequential air–1% H_2 (v/v)–air–1% CO (v/v)–air cycles at 330 °C. It is shown that only 1% v/v H_2 induces a measurable and reversible transmittance variation, with a relative transmittance level (Tr_{H_2}/Tr_{air}) increasing from 1 to 1.93, thus doubling the transmittance in air. Moreover, it is demonstrated that interference by CO is essentially eliminated. This provides an example of selectivity tuning made possible in optical gas-sensing materials which possess a strong wavelength dependence of optical transmittance change induced by different gas species.

Accuracy of the detected gas concentration is described by T_{90}, a parameter that indicates the amount of time that the sensor requires to reach 90% of the equilibrium signal after a gas concentration variation. The T_{90} value for CO detection is 2.3 min, while for H_2 it is 2.1 min. Values of the same order of magnitude were estimated for signal baseline recovery after gas evacuation from the testing chamber.

The H_2 detection mechanism is perhaps specific to the system Au–NiO described here, as studies determining the H_2 effects upon optical properties of other Au–metal oxides

Table 2. Sensing performance of different H_2 optical sensors described in the literature compared to that described in the present work. Values have been estimated at best operative conditions for each material.

Material	Operative temperature (°C)	Absolute ΔA value	Reference
Au–Co_3O_4	200	0.0075	[9, 25]
Au–WO_3	250	0.011	[30]
Au–$In_xO_yN_z$	300	0.011	[22]
SiO_2–NiO–Au	300	0.3	Present work

systems, such as Au–Co_3O_4 [9, 25], Au–WO_3 [30] and Au–$In_xO_yN_z$ [22], report that H_2 exposure causes an increase of optical absorption in SPR frequencies together with no substantial change in SPR band maximum wavelength, with the exception of a slight shift described in [22]. These observations are collected for comparison in table 1, and are in contrast to those described herein, which reports a H_2-induced decrease of optical absorbance at SPR frequencies together with a marked shift in SPR band maximum wavelength. Moreover, when comparing the sensing performance of the materials described in the literature, the sensitivity to H_2 of the SiO_2–NiO–Au films presented here is substantially higher, as highlighted in table 2. Further studies are in progress to help elucidate the key parameters of Au–NiO transmittance modulation.

4. Conclusions

SiO_2 films containing NiO and different concentrations of Au nanoparticles were synthesized using the sol–gel technique. Structural characterization demonstrated the formation of metallic gold nanoparticles together with crystalline NiO aggregates inside the SiO_2 network. The presence of Au nanoparticles surrounded by NiO aggregates affects the film's optical properties, which is an exploitable feature in optical gas sensing. A change in the optical transmittance of films was observed after exposure to CO and H_2 at different temperatures, with noticeable differences in the detected transmittance change ratio (OTCR). The major anomalies were observed in the spectral region in which the SPR band of Au nanoparticles is excited (500–650 nm). CO induced an increase of the overall optical transmittance in the whole visible region, but with a clear depression of OTCR values in the SPR

frequency range (leading to negative OTCR values for higher gold contents), while H_2 induced a large increase in OTCR in the same spectral region. In addition, a shift in the SPR band position was observed in the case of H_2 exposure, which was not found for CO, thus indicating a different detection mechanism for the two species. The wavelength dependence of OTCR has be exploited to tailor the film's selectivity towards the detection of H_2 with reduced CO interference. For a film containing 6% Au and at 570 nm wavelength, H_2 was detected by monitoring the transmittance change, while for CO the change was negligible.

Acknowledgment

This work was supported by MURST within a 'Progetto di Ateneo n. CPDA042175' Project of the Padova University.

References

[1] Shi J, Zhu Y, Zhang X, Baeyens W R G and García-Campaña A M 2004 *Tr. Anal. Chem.* **23** 351
[2] Ando M, Kobayashi T and Haruta M 1994 *Chem. Soc. Faraday Trans.* **90** 1011
[3] Eguchi K 1992 *Gas Sensors* ed G Sberveglieri (Dordrecht: Kluwer) p 307
[4] Buso D, Guglielmi M, Martucci A, Mattei G, Mazzoldi P, Sada C and Post M L 2006 *Nanotechnology* **17** 2429
[5] Zhan Z, Jiang D and Xu J 2005 *Mater. Chem. Phys.* **90** 250
[6] Wada K and Egashira M 1998 *Sensors Actuators* B **53** 147
[7] Hyodo T, Baba Y, Wada K, Shimizu Y and Egashira M 2000 *Sensors Actuators* B **64** 175
[8] Yamazoe N, Muta Y and Seiyama T 1984 *J. Surf. Sci. Soc. Japan* **5** 241
[9] Ando M, Kobayashi T, Iijima S and Haruta M 1997 *J. Mater. Chem.* **7** 1779
[10] Almeida R M and Pantano C G 1990 *J. Appl. Phys.* **68** 4225
[11] Primeau N, Vautey C and Langlet M 1997 *Thin Solid Films* **310** 47
[12] Vallée C, Goullet A, Granire A, van der Lee A, Durand J and Marlière C 2000 *J. Non Cryst. Solids* **272** 163
[13] Galeener F G 1979 *Phys. Rev.* B **19** 4292
[14] Daniel M C and Astruc D 2004 *Chem. Rev.* **104** 293
[15] Buso D, Pacifico J, Martucci A and Mulvaney P 2007 *Adv. Funct. Mater* **17** 347
[16] Johnson P B and Christy R W 1972 *Phys. Rev.* B **6–12** 4370
[17] Nakamura K, Kawabata T and Mori Y 2003 *Powder Technol.* **131** 120
[18] Pérez-Juste J, Pastoriza-Santos I, Liz-Marzán L M and Mulvaney P 2005 *Coordin. Chem. Rev.* **249** 1870
[19] Scaffardi L B, Pellegri N, de Sanctis O and Tocho J O 2005 *Nanotechnology* **16** 158
[20] Rao K V and Smakula A 1965 *J. Appl. Phys.* **36** 2031
[21] Powell R J and Spicer W E 1970 *Phys. Rev.* B **2–6** 2182
[22] Ando M, Steffes H, Chabicovsky R, Haruta M and Stangl G 2004 *IEEE Sens. J.* **4** 232
[23] Ando M, Kobayashi T, Iijima S and Haruta M 2003 *Sensors Actuators* B **96** 589
[24] Haruta M, Yamada N, Kobayashi T and Iijima S 1989 *J. Catal.* **115** 301
[25] Ando M, Kobayashi T and Haruta M 1997 *Cat. Today* **36** 135
[26] Mattei G, Mazzoldi P, Post M L, Buso D, Guglielmi M and Martucci A 2007 *Adv. Mater.* **19** 561
[27] Matsubara K, Kawata S and Minami S 1988 *Process Appl. Spectrosc.* **42** 1375
[28] Ando M, Zehetner J, Kobayashi T and Haruta M 1996 *Sensors Actuators* B **35/36** 513
[29] Kobayashi T, Haruta M and Ando M 1993 *Sensors Actuators* B **13/14** 545
[30] Ando M, Chabicovsky R and Haruta M 2001 *Sensors Actuators* B **76** 13